14th European Signal Processing Conference (EUSIPCO 2006), Florence, Italy, September 4-8, 2006, copyright by EURASIP

REAL-TIME EXPERIMENTS ON CHANNEL ADAPTIVE TRANSMISSION IN THE MULTI-USER UP-LINK AT VERY HIGH DATA RATES USING MIMO-OFDM

T. Haustein[†]*, A. Forck*[††]*, H. Gäbler*[††]*, V. Jungnickel*[††] *and S. Schiffermüller*[††]

[†]Siemens AG Munich, Communications Mobile Networks, Future Radio Concepts
Werinherstrasse 91, D-81541 Munich, Germany
email: thomas.haustein@siemens.com
[††] Fraunhofer Institute for Telecommunications Heinrich-Hertz-Institut,
Einsteinufer 37, D-10587 Berlin, Germany
email: {forck, gaebler, jungnickel, schiffermueller}@.hhi.de

SPECIAL SESSION - INVITED

ABSTRACT

In this paper we focus on channel adaptive transmission in the multi-user OFDM Uplink where the base station uses multiple antennas. The additional degree of freedom in space requires extra signal processing effort which becomes challenging especially for a high data rate implementation in real-time.

Our MIMO-OFDM experimental system which is capable to transmit data rates beyond 1 Gbit/s, was enhanced by adaptive resource allocation, where the modulation on each antenna and each sub-carrier was controlled by a narrow-band feed-back channel.

We present experimental results for the total rate achieved at the base station and the individual rates per user terminal in line-of-sight and non-line-of-sight scenarios. We compare the rates expected from theory on the measured indoor channels with rates achieved in the experiments.

1. INTRODUCTION

To satisfy the growing demand of higher data throughput under the constraint of limited available bandwidth, multi-antenna (MIMO) systems offer the possibility of spatial multiplexing which enables very high spectral efficiencies [1]. MIMO systems exploit distinguishable spatial signatures from the antenna pairs and try to collect as many multi-path signals as possible. When extending the transmission bandwidth in order to allow higher data rates the multi-path channel becomes increasingly frequency selective. By using appropriate schemes we can handle and exploit this frequency selective nature of the channel to improve the system performance.

From the perspective of implementation complexity OFDM is a very prominent waveform for broadband high data rate transmission for the near future [2]. The block diagonal structure of the equivalent base band transmission channel with OFDM using a cyclic prefix forms D parallel narrow-band OFDM sub-channels in the frequency domain and the spatial correlation between the multiple antennas can be dealt with by an appropriate MIMO signal processing [3]. The resulting radio resources available for data transmission span a space of dimension $n_T \times D_m$ in each time slot where n_T are the number of simultaneously transmitting antennas and D_m denotes the number of OFDM tones available for data transport. In a multi-user transmission scenario these resources in the spatial and frequency domain have to be shared among all users.

If the quality of the radio resources is known at a radio resource management (RRM) unit prior to data transmission we can exploit this knowledge in order to schedule the data transmission in time, space and frequency such that all users or transmission links are scheduled on their most reliable resources. In case of the availability of additional information from higher layers e.g. individual user rate requests, tolerable delays or BER targets the whole system can be optimized in a cross-layer approach in order to maximize system stability [4] and to support quality of service (QoS) parameters [5] in wireless transmissions which becomes a more and more relevant topic for service providers.

In the case of multi-user SISO-OFDM e.g.[6] showed that opportunistic scheduling with OFDMA and water filling in the frequency domain achieves the highest sum capacity and several algorithms are known to find the rate optimum solution [7, 8]. In the multi-antenna case the complexity increases significantly due to the combinatorial nature of the problem but the rate optimum solution can still be found by convex optimization [9]. This becomes computationally very demanding even for moderate numbers of sub-carriers and users.

Under the assumption of a fixed transmit power per sub-carrier and transmit antenna the problem can be separated in parallel spatial scheduling optimization problems which can be solved at reduced complexity. The available radio resources are entangled in space and the achievable signal-to-noise-plus-interference-ratio (SINR) with a specific MIMO detector can be calculated for each OFDM tone. Assuming the SINR for each resource is known or can be predicted for the next transmission frame we can choose the highest coded modulation which satisfies a targeted bit-error-rate (BER). Implementations of such channel adaptive transmission schemes for the single carrier case [10, 11] showed higher link stability and reliable target BERs to be met on all resources. [12, 13] showed a real-time implementation of channel and QoS aware multi-user SIMO scheduling, exemplarily for the flat-fading channel.

The last papers showed that channel aware transmission using adaptive modulation is a key feature to enable efficient and QoS supporting resource scheduling in MIMO systems. In this paper we focus on MIMO-OFDM and channel adaptive bit-loading per antenna and per sub-carrier. We show that a real-time implementation is feasible also at very high data rates.

The paper is organized as follows. After a short introduction into the implementation relevant parts of MIMO-OFDM we explain how the adaptive transmission scheme is realized in the real-time system. We will then revisit the architecture of the real-time testbed and the last section is dedicated to the experimental results to illustrate the discussed advantages of channel adaptive transmission.

2. MIMO-OFDM

We consider the uplink of an OFDM system with n_T transmit antennas and a base station having m_R antennas. We assume perfect frame and symbol synchronization. The transmission channel between all antenna pairs is a frequency selective Rayleigh block fading channel of order L. Using OFDM techniques the channel can be decomposed into D flat sub-channels. Hence, using Fourier Transform (FFT) the received signal at k-th sub-carrier is given by a flat fading MIMO equation

$$\mathbf{y}_k = \mathbf{H}_k \mathbf{x}_k + \mathbf{n}_k, \tag{1}$$

where $\mathbf{x}_k^{n_T\times 1}$ is a zero-mean transmit vector on sub-carrier k, $\mathbf{H}_k^{m_R\times n_T}$ the k-th MIMO channel matrix and $\mathbf{n}_k^{m_R\times 1}$ is circular symmetric zero-mean additive white Gaussian noise with $\mathbb{E}[\mathbf{n}_k\mathbf{n}_k^H] = \sigma_N^2\mathbf{I}$, where $(\cdot)^H$ denotes the conjugate transpose, σ_N^2 the noise variance and $\mathbb{E}[\cdot]$ the expectation. A cyclic prefix (CP) of length $L_{CP} > L$ assures orthogonality between OFDM symbols.

In an up-link scenario with K transmit antennas or users we assume a Minimum-Mean-Squared-Error (MMSE) filter at the receive side for the spatial separation of the multiplexed data. The receive processing is performed in the frequency domain on a sub-carrier by sub-carrier basis. For the sake of a more convenient notation we will omit the index denoting the sub-carrier number but keep in mind that like the channel vector $\mathbf{h}_i$ all other parameters (e.g. beam-former, transmit power and SINR) are also frequency depending. The resulting up-link (UL) SINR for user/antenna i at a particular sub-carrier m can be expressed as

$$\begin{aligned}\mathrm{SINR}_i^{\mathrm{UL}}(\mathbf{u}_i, p_1, ..., p_K) &= \frac{p_i \mid \mathbf{u}_i^H\mathbf{h}_i \mid^2}{\mathbf{u}_i^H\mathbf{Z}_i(\mathbf{p})\mathbf{u}_i}, \qquad (2)\\ \text{with } \mathbf{Z}_i(\mathbf{p}) &= \sigma_N^2\mathbf{I} + \sum_{\substack{k=1\\k\neq i}}^{K} p_k\mathbf{h}_k\mathbf{h}_k^H.\end{aligned}$$

For given transmission powers $p_1...p_K$, the SINR_i from (2) are individually maximized by the normalized MMSE solution

$$\mathbf{u}_i^{opt} = \alpha\mathbf{Z}_i(\mathbf{p})^{-1}\mathbf{h}_i,$$

where α is chosen such that $\parallel \mathbf{u}_i^{opt} \parallel = 1$. We substitute $\mathbf{u}_i^{opt}$

$$\mathrm{SINR}_i^{\text{UL-MMSE}}(p_1...p_K) = p_i\mathbf{h}_i^*\mathbf{Z}_i(\mathbf{p})^{-1}\mathbf{h}_i.$$

which in case of a linear MMSE (LMMSE) receiver results in

$$\mathrm{SINR}_i^{\mathrm{LMMSE}}(p_1...p_K) = p_i\mathbf{h}_i^H[\sigma_N^2\mathbf{I} + \sum_{\substack{k=1\\k\neq i}}^{K} p_k\mathbf{h}_k\mathbf{h}_k^H]^{-1}\mathbf{h}_i. \quad (3)$$

We assume a per antenna power limit and equal power distribution over the sub-carriers in order to reduce the feed-back rate and to facilitate limited peak-to-average-power-ratios in the DFT and IDFT.

The $\mathrm{SINR}_i^{\mathrm{LMMSE}}$ from (3) will be used as steering parameter to control the level of adaptive modulation and coding in order to assure targeted uncoded BERs which can be matched with the optimum working point for the FEC decoder.

For the high data rate experiments with 1 Gbit/s transmission rate we used a LMMSE detector. Recent works [10, 11] showed results on BER and throughput performance with MMSE-SIC[1] in a single carrier MIMO system with spectral efficiencies above 20 bit/s/Hz in 1 MHz bandwidth. The high signal processing rate at the symbol clock rate of 100 MHz in the FPGA did not allow SIC implementation in one Virtex-II FPGA.

In practical terms we will obtain the estimates of the data vector $\hat{\mathbf{x}}$ by multiplying the receive vector $\mathbf{y}$ with the MMSE-pseudo-inverse ($m_R \geq n_T$) of the measured transmission channel

$$\hat{\mathbf{x}} = \mathbf{H}_{MMSE}^{\dagger}\cdot\mathbf{y} = \mathbf{H}_{MMSE}^{\dagger}\cdot\mathbf{H}\cdot\mathbf{x} + \mathbf{H}_{MMSE}^{\dagger}\cdot\mathbf{n}.$$

where the MMSE pseudo-inverse $\mathbf{H}_{\mathrm{MMSE}}^{\dagger}$ reads

$$\mathbf{H}_{MMSE}^{\dagger} = \mathbf{H}^{\mathbf{H}}(\mathbf{H}\mathbf{H}^{\mathbf{H}} + \sigma_N^2 I)^{-1}$$

and the noise variance σ_N^2 is assumed to be the same for all receivers for a more convenient notation. Note, that in general we have to expect different noise variances for each receiver if e.g. independent automatic gain controls are used. $\mathbf{H}^{\dagger}\mathbf{n}$ denotes the noise enhancement due to the linear filter.

Keeping in mind that the computational effort of multiplications and inversions increases with cubic order in $N = \max(n_T, m_R)$ we choose a dimension reduced formulation of the MMSE.

$$\text{reduced MMSE: } \mathbf{H}_{MMSE}^{\dagger} = (\mathbf{H}^H\mathbf{H} + \tilde{\sigma}_N^2\mathbf{I})^{-1}\mathbf{H}^H,$$

where $\tilde{\sigma}_N^2$ is now the equivalent noise per data stream.

From the perspective of implementation it has to be noted that for noticeable noise at the receive antennas (low SNR range) the MMSE filter does not scale the data signals properly to unity which has to be considered for higher QAM levels. This is due to

$$\begin{aligned}\mathbf{H}_{ZF}^{\dagger}\cdot\mathbf{H} &= [(\mathbf{H}^H\mathbf{H})^{-1}\mathbf{H}^H]\cdot\mathbf{H} = \mathbf{I}, \text{ and}\\ \mathbf{H}_{MMSE}^{\dagger}\cdot\mathbf{H} &= [(\sigma_N^2\mathbf{I} + \mathbf{H}^H\mathbf{H})^{-1}\mathbf{H}^H]\cdot\mathbf{H} \neq \mathbf{I}\end{aligned}$$

where $\mathrm{diag}\left[\mathbf{H}_{MMSE}^{\dagger}\cdot\mathbf{H}\right]$ gives the element-wise final scaling values of the reconstructed data vector $|\hat{x}_i|^2 \leq |x_i|^2$ which can be significantly smaller than the original data symbol if detected at low SNR. The off-diagonal elements of $\left[\mathbf{H}_{MMSE}^{\dagger}\cdot\mathbf{H}\right]$ represent the residual inter stream interference induced by the MMSE solution. Finally, we have to scale all rows $\mathbf{h}_{MMSE}^{\dagger k}$ of $\mathbf{H}_{MMSE}^{\dagger}$ by

$$\mathbf{h}_{MMSE\,scaled}^{\dagger k} = \frac{1}{\left[\mathbf{H}_{MMSE}^{\dagger}\cdot\mathbf{H}\right]_{kk}}\cdot\mathbf{h}_{MMSE}^{\dagger k}$$

in order to reconstruct the data properly to the decision thresholds of a e.g. hard-decision M-QAM demodulator, the superscript $\mathbf{h}^{\dagger k}$ denotes the k-th row of $\mathbf{H}^{\dagger}$.

3. CHANNEL ADAPTIVE TRANSMISSION

3.1 Rate Adaptation Techniques

Current OFDM transmission schemes like 802.11a/b/g are mainly operated in static or quasi-static propagation environments due to the limited mobility in indoor environments. The link adaptation mode is selected by measuring the average SNR per receive antenna. Based on this average value a common coded modulation level is chosen for all sub-carriers and stepwise lowered if the package error rate (PER) is too high due to severe channel fades or mobility (Doppler). Using this common coding and modulation the throughput performance is determined by the most degraded sub-carriers which will dominate the BER performance. With MIMO processing comes the aspect of singular spatial channels, where the channel vectors $\mathbf{h}_k$ at each sub-carrier have non-vanishing entries but are close to parallel which makes linear separation techniques very inefficient due to significant noise enhancement.

[14] proposed to control the adaptive modulation and coding based on average SNR achieved with a particular MIMO detector and additionally an indicator which gives information about the spectral variance of the SNR. This approach predicts the appropriate coded modulation much better than the average SNR per Rx antenna, but the BER performance is still limited by the worst sub-carriers due to the common modulation scheme on all sub-carriers.

We follow a different strategy of link adaptation for the experiments, which allows maximum granularity in resource allocation in the spatial and frequency domain. The idea is to calculate the actual SINRs after the MIMO detector for all OFDM sub-carriers and to choose the coded modulation from a look-up table supporting a target BER on all resources. This concept results in a time variant throughput but the working point for the FEC can be controlled and assured. In the context of multi-user communication this allows flexible resource allocation for different users and QoS parameters (average rate, BER etc) can be supported. In case of very high

[1] SIC: Successive Interference Cancellation

sub-carrier numbers adjacent sub-carriers may have similar channel quality and can be bundled for resource allocation purposes and the signalling can be reduced accordingly.

For different transmission schemes the relevant bit-loading parameter is given in the following table and has to be interpreted in a per sub-carrier manner when combined with OFDM where UL and DL denote up-link and down-link, respectively.

Transmission-Scheme	Transmit-Processing	Receive-Processing	Bit-loading Parameter
PARC / Multi-user UL	$\mathbf{I}$	ZF / MMSE: $\mathbf{H}^{\dagger}$ SIC: $\mathbf{GF}, \mathbf{B}-\mathbf{I}$	$\mathrm{diag}(\mathbf{H}^{\dagger}\cdot\mathbf{H}^{\dagger T})$ $(\mathrm{diag}(\mathbf{L}))^{-2}$ (QLD)
SVD-MIMO (UL/DL)	$\mathbf{V}$	$\mathbf{U}^{T}\cdot\mathbf{D}^{-1}$	$\mathrm{diag}(D^{-2})$ (SVD)
ACI / JT (DL)	$\mathbf{H}^{\dagger}/\alpha$	$\alpha\cdot\mathbf{I}$	α^2 from 12-bit-DAC scaling

Table 1: Transmission modes of Test-bed: PARC: Per Antenna Rate Control, QLD: QL-decomposition, SVD: Singular Value Decomposition, ACI: Adaptive Channel Inversion, JT: Joint Transmission

3.2 Multi-User Resource Allocation

The concept of MIMO signal processing can also be applied in the case of multi-user up-link scenarios with one Tx antenna per mobile terminal. We aim for total throughput maximization at the base station with individual power constraint per Tx antenna and equal power allocation over all OFDM tones. Then the problem of opportunistic resource allocation reduces to a simple opportunistic bit-loading strategy for the case of less or an equal number of users than the number of BS antennas $K \leq m_R$ which was applied for the experiments.

The $[m_R \times K]^m$ channel matrix for each OFDM tone m can be treated separately with regard to resource allocation between the K users. Since we assume a multi-user scenario we aim for maximum multiplexing on each sub-carrier if the channel permits. The algorithm works roughly the following:

1. Calculate the $SINR_i^m$ or noise plus interference enhancement $(\frac{1}{SINR_i^m})$ for each user i at the m-th tone with the applied MIMO detector according to table above.
2. Use look-up table to determine supportable modulation level for target BER.
3. If one stream or a few can not support BPSK, switch off the stream with the highest noise enhancement and delete belonging column in the $[m_R \times K]^m$ MIMO matrix.
4. Repeat with reduced MIMO matrices until all remaining streams are loaded.

The results for the 2-user case for particular sub-carriers are depicted in Fig. 1.

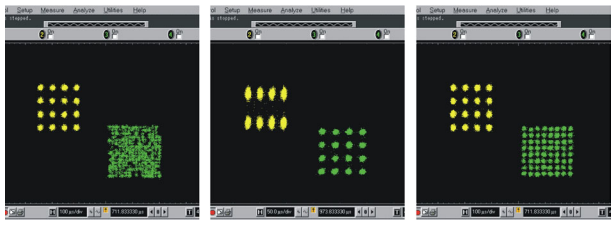

Figure 1: Screen shots of reconstructed data symbols for user 1 (yellow) and user 2 (green) at specific sub-carriers. Modulations used were 2-16 PAM, left: 16-QAM and 256-QAM as highest modulation level. middle: As an intermediate between QPSK and 16-QAM, 8-QAM is somtimes used. right: 16-QAM and 64-QAM. MIMO-OFDM transmission 2 Tx $\times$4 Rx in 100 MHz channel in indoor scenario with 116 data tones out of 128.

4. REAL-TIME MIMO-OFDM TEST-BED

A first over the air transmission experiment with more than 1 Gbit/s [15, 16] was operated at 5.2 GHz in a bandwidth of 100 MHz, used 3 Tx and 5 Rx antennas and 64-QAM on all data sub-carriers. BER measurements in an office scenario with coded and uncoded transmission are depicted in Fig. 2. We clearly see that in case of sufficient receive diversity which causes a kind of channel hardening we observe that for uncoded BER below 10^{-2} the Viterby-Decoder achieves close to error free detection. The impressive link stability

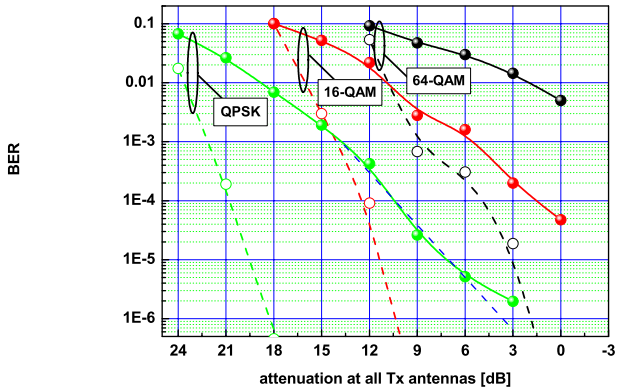

Figure 2: Measured BERs on the Gigabit transmission link using QPSK, 16-QAM or 64-QAM on all 48 data sub-carriers. Coded (solid line) and uncoded (dashed line) BER for first Tx antenna is depicted. 3×5 MIMO-OFDM with 100 MHz bandwidth.

of the Gigabit-Test-bed with a simple linear MMSE MIMO detector was achieved by two additional receive antennas. The achieved diversity slope $\beta = \frac{\log BER}{\log SNR} = m_R - n_T + 1$ was 3 with 3×5 antennas, one data stream per transmit antenna and a linear MMSE receiver.

After a correlation based channel estimation in the frequency domain on all sub-carriers a DSP calculates all MMSE filters and performs adaptive bit-loading. The whole digital signal processing works on three different time scales.

- Fast matrix $\times$ vector multiplications for data symbol reconstruction are done in the FPGA at symbol rate of 100 MHz.
- Calculation of MIMO filters in a DSP every frame (500 Hz).
- Adaptive bit-loading every 10-100 OFDM frames (5-50 Hz).

The signal processing uses real values which doubles the computational complexity in the DSP and the MMSE filter matrices in the FPGA have now size $2m_R \times 2n_T$ for each sub-carrier, but all algorithms developed for the single carrier test-bed could be reused unaltered. With OFDM I/Q imbalances at the mixers will cause image carrier leakage which can be measured by using orthogonal sequences in the lower and upper sideband.

For the initial experiments the terminal to BS synchronization and the feedback link for the modulation vector were realized by cable. This temporary solution limited mobility but was recently replaced by over the air frame synchronization, CFO estimation and completed by individual carrier phase tracking per user. The feedback channel with maximum granularity of individual modulation for I and Q and for each antenna requires $\frac{3\cdot 2\cdot n_T\cdot D_m \mathrm{bits}}{50\mathrm{ms}} = 27.8$ kbit/s. This feedback rate can be halved when using the same modulation in I and Q and furthermore with sub-carriers bundling.

The channel estimates and the bit-loading vector can be stored on a hard disc for off-line analysis of the experiments.

5. EXPERIMENTAL RESULTS

5.1 Experimental Setup

The two transmit antennas where put at a fixed position 30 cm off the wall at the same height as the BS antennas. The transmitter where close together and transmitted omni-directional beam pattern with orthogonal polarization. In order to achieve sufficient channel statistic and reproducible channel states the BS antennas where mounted on a tripod with wheels and was moved 3.35 meters along rails across the lab which has size LxHxB: 6m x 3m x 4m. The speed was 18 mm/s to guarantee quasi-static channel conditions over the OFDM frame length of 2 ms which to be comparable with block-fading simulations. The phase-tracking was switched off and perfect sync by cable was used instead.

The transmitters where set to a fixed Tx power of 10.1 dBm and 6.9 dBm feeded into the antenna cables such that no PAPR degradation was to be seen at the Rx along the whole measurement track. The AGC at the Rx was set to a fixed value in order to separate the effect from line-of-sight (LOS) and non-line-of-sight (NLOS) scenarios.

For the LOS measurements there was LOS at least between one of the two Tx antennas and two Rx antennas. For the NLOS scenario we blocked the LOS with an radio wave absorbing mattress such that there was no direct LOS along the whole track.

5.2 Throughput with 2 by 2 MIMO-OFDM

Fig. 3 depicts the measured throughput for user A and user B and the sum throughput along the track in the lab using 2 Rx antennas at the BS. The symmetric antenna configuration causes singular channels rather frequently, such that the system often has to switch to maximum ratio combining for the respective OFDM tones and the individual user rates and the total rate at the BS will be reduced. Since the decision on which user to sacrifice at a particular sub-carrier is done independently on each sub-carrier in an opportunistic way the resulting individual rate for one user can become quite low as observed in Fig. 6 where user B was switched off in most parts of the spectrum and the rate falls significantly below 50 Mbit/s. This effect becomes more prominent as soon as one user suffers a significant stronger attenuation due to longer distance to the BS. This fairness problem can be solved by e.g. queue-aware resource allocation used in cross-layer optimized scheduling approaches for radio resource management. This can also be done in real-time as shown in [12].

5.3 Throughput Measurements with Diversity Reception

Fig. 4 shows the empirical cdf of the measured sum throughput at the BS (left) and what can be predicted as maximum sum capacity obtained from the measured channel in the lab (right). We clearly see that the additional power from the LOS (Rician factor between 3-7 dB) significantly increases the overall achievable throughput. Furthermore, we can see that the diversity receive antennas 3 and 4 stabilize the link significantly since the chances of singularities in the transmission channel are reduced tremendously and therefore increase the average throughput almost by a factor of 2 at least for the NLOS case. When compared with capacity simulation results on the measured channels we find a good match of the theoretically expected sum rate distribution and our measurement results. The gap between simulation curves and the measurement results are due to the SNR gap with a BER target of $\leq 10^{-3}$ and uncoded transmission with M-QAM symbols. The shorter tails at low rates can be explained because the lowest rate to be loaded is 1 bit while the capacity allows real values to be valid.

Fig. 5 shows a screen shot from the GUI of the test-bed which is used to display the actually allocated resources and modulations. For a very good channel we could achieve more than 1 Gbit/s with 2 Tx antennas, 116 data sub-carriers in 100 MHz bandwidth and 256-QAM as highest modulation level which was loaded on most of the spectrum in this particular channel. Note, the lower modulation levels at the side bands of the OFDM spectrum. This is caused by the analog filters at the transmit and receive side which cause SNR degradation on those sub-carriers. With channel aware bit-loading those systematically SNR-degraded sub-carriers can also be used for reliable data transmission which would not be possible for a standard WLAN-OFDM system which uses a common modulation on all sub-carriers, of course spectrum mask issues must be fulfilled.

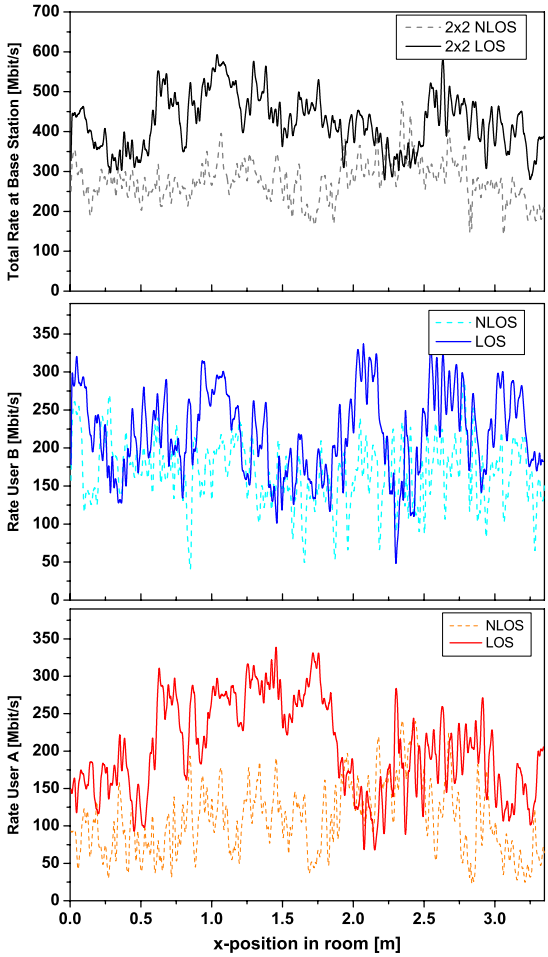

Figure 3: Measured sum rates for user A and B along the measurement track in the lab. Adaptive modulation per sub-carrier with equal power allocation per tone. Opportunistic resource allocation and loading, BER$\leq 10^{-3}$.

6. CONCLUSIONS

We showed a real-time implementation of channel adaptive multi-user resource allocation and link adaptation using MIMO-OFDM on a reconfigurable hardware test-bed. The experiments with a 2-user office scenario showed a very stable transmission with variable sum rate at the base station. In particular, our approach guarantees a constant BER over all resources in the space frequency domain. With 2 additional receive antennas a significant channel hardening is achieved which allowed to transmit more than 1 Gbit/s gross data rate with just 2 transmit antennas. The measured throughput agreed well with simulations on the measured channels in the lab. Our results clearly indicate that channel adaptive link adaptation on each antenna and OFDM sub-carrier is a key issue to achieve reliable transmission especially in symmetric antenna configurations as shown for the 2 by 2 MIMO case.

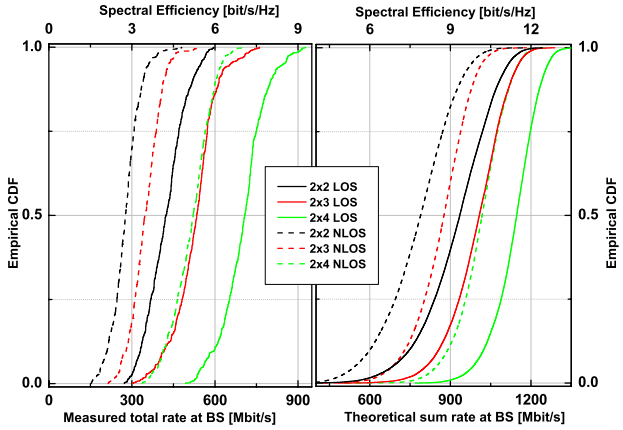

Figure 4: Empirical cdfs of the measured total throughput at the base station with uncoded transmission (left) and the predicted sum rate calculated from the measured channels (right) in the lab with and w/o LOS.

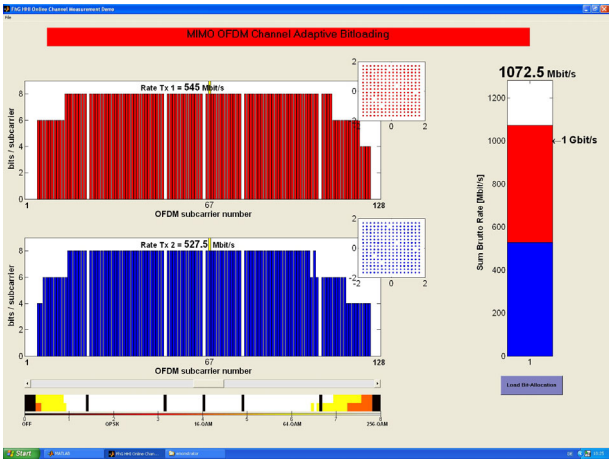

Figure 5: Measured rates for user A and B in a very good channel achieving Gbits/s transmission rate with 2 Tx and 4 Rx antennas, and adaptive bit-loading per sub-carrier with maximum 256-QAM. Antennas and AGC where manually adjusted to optimize the channel throughput.

REFERENCES

[1] G.J. Foschini, "Layered space-time architecture for wireless communication in a fading environment when using multiple antennas," *Bell Labs Tech. J.*, pp. pp. 41–59, 1996.

[2] J.A.C. Bingham, "Multicarrier modulation for data transmission: An idea whose time has come," *IEEE Communications Magazine*, vol. 28, no. 5, pp. 5–14, May 1990.

[3] A. J. Paulraj, D. Gore, R. U. Nabar, and H. Bölcskei, "An overview of MIMO communications - a key to gigabit wireless," *Proceedings IEEE*, vol. 92, no. 2, pp. 198–218, 2003.

[4] H. Boche and M. Wiczanowski, "Stability-Optimal Transmission Policy for Multiple Antenna Multiple Access Channel in the Geometric View," *EURASIP Signal Processing Journal, Special Issue on Advances in Signal Processing-assisted Cross-layer Designs*, 2006, to appear.

[5] M. Wiczanowski H. Boche and S. Stanczak, "Characterization of Optimal Resource Allocation in Cellular Networks," *IEEE Workshop on Signal Processing Advances in Wireless Communications*, July 2004.

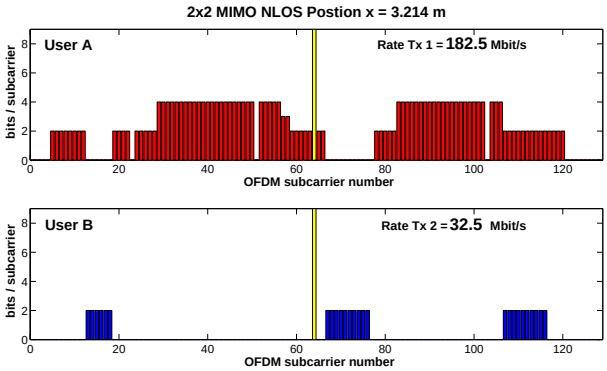

Figure 6: Measured rates for user A and B in a rank degraded channel where the scheduler switches to maximum ratio combining in 80% of the spectrum. Opportunistic sub-carrier allocation and bit-loading disadvantages user A in order to maximize the total throughput at the base station. Yellow bar indicates position of center frequency carrier.

[6] S. Verdu R.S. Cheng, "Gaussian Multiaccess Channels with ISI: Capacity Region and Multiuser Water-filling," *IEEE Trans. on Information Theory*, vol. 39, no. 3, May 1993.

[7] H. Liu H. Yin, "An Efficient Multiuser Loading Algorithm for OFDM-based Broadband Wireless Systems," *IEEE GLOBECOM 2000*, , no. 1, pp. 103–107, Nov. 2000.

[8] J. Speidel G. Münz, S. Pfletschinger, "An Efficient Waterfilling Algorithm for Multiple Access OFDM," *IEEE GLOBECOM'02, Taipei, Taiwan*, Nov. 2002.

[9] T. Michel and G. Wunder, "Optimal And Low Complexity Suboptimal Transmission Schemes for MIMO-OFDM Broadcast Channels," in *Proc. IEEE Intern. Conf. on Communications (ICC '05)*, Seoul, Korea, May 2005.

[10] T. Haustein, A. Forck, H. Gäbler, and S. Schiffermüller, "From Theory to Practice: MIMO Real-Time Experiments of Adaptive Bit-loading with linear and non-linear Transmission and Detection Schemes.," in *IEEE VTC Spring, Stockholm, Sweden.*, May 2005.

[11] T. Haustein, A. Forck, H. Gäbler, V. Jungnickel, and S. Schiffermüller, "Real Time Signal Processing for Multi-Antenna Systems: Algorithms, Optimization and Implementation on an Experimental Test-bed," *will appear in EURASIP - special issue on Implementation Aspects and Test-beds for MIMO Systems*, 2006.

[12] T. Haustein, A. Forck, H. Gäbler, C.v. Helmolt, V. Jungnickel, and U. Krueger, "Implementation of Channel Aware Scheduling and Bit-Loading for the Multiuser SIMO MAC in a Real-Time Demonstration Test-bed at high Data Rate," in *IEEE VTC Fall, Los Angeles, C.A., U.S.A.*, Sept. 2004.

[13] T. Haustein, H. Boche, M. Wiszanowski, and E. Schulz., "Real-Time Implementation of Cross-Layer Optimization: Multi-Antenna High Speed Uplink Packet Access," in *IEEE ICASSP, Philadelphia, U.S.A.*, March 19-23th 2005.

[14] Matthias Lampe, *Adaptive Techniques for Modulation and Channel Coding in OFDM Communication Systems*, Ph.D. thesis, Technical University Hamburg-Harburg, Germany, April 2004.

[15] V. Jungnickel, A. Forck, T. Haustein, S. Schiffermüller, C. von Helmolt, F. Luhn, M. Pollock, C. Juchems, M. Lampe, W. Zirwas J. Eichinger, and E. Schulz, "1 Gbit/s MIMO-OFDM Transmission Experiments," in *IEEE VTC Fall, Dallas,TX, U.S.A.*, Sept. 25th-28th 2005.

[16] V. Jungnickel, T. Haustein, A. Forck, S. Schiffermueller, H. Gaebler, C. v. Helmolt, W. Zirwas, J. Eichinger, and E. Schulz, "Real-Time Concepts for MIMO-OFDM," in *IEEE Global Mobile Congress*, Shanghai, China, Oct. 11-13 2004.